

# The B–H···H–P Dihydrogen Bonding in Ion Pair Complexes $[(CF_3)_3BH^-][HPH_{3-n}(Me)_n^+]$ ( $n = 0–3$ ) and Its Implication in $H_2$ Elimination and Activation Reactions

Shulin Gao,<sup>†</sup> Wei Wu,<sup>\*,†</sup> and Yirong Mo<sup>\*,‡</sup>

State Key Laboratory of Physical Chemistry of Solid Surfaces and College of Chemistry and Chemical Engineering, Xiamen University, Xiamen, Fujian 361005, China, and Department of Chemistry, Western Michigan University, Kalamazoo, Michigan 49008

Received: April 2, 2009; Revised Manuscript Received: May 31, 2009

The B–H<sup>δ-</sup>···H<sup>δ+</sup>–P dihydrogen bonding (DHB) in ion pair complexes  $[(CF_3)_3BH^-][HPH_{3-n}(Me)_n^+]$  ( $n = 0–3$ ) and its role in the combination of proton and hydride with the release of  $H_2$  or, reversibly, the heterolytic activation of  $H_2$  by Lewis pairs  $(CF_3)_3BPH_{3-n}(Me)_n$  have been theoretically investigated at the MP2 and DFT levels. It is found that the B–H···H–P bonds behave similarly to those in neutral pairs and ion–molecule complexes in most respects, such as the linearity of the H···H–P moiety, the characteristics of the electron transfer and rearrangement, and the topological properties of the DHB critical point, except that in certain cases, a blue-shifting of the H-bond vibrational frequency is observed. In  $[(CF_3)_3BH^-][HPH_{3-n}(Me)_n^+]$ , the proton shifting within the complexes leads to the formation of the dihydrogen complex  $B(CF_3)_3(\eta^2-H_2)$ , which is followed by a subsequent  $H_2$  release. The stability of  $B(CF_3)_3(\eta^2-H_2)$  ( $D_0/D_0 = 10.8/6.0$  kcal/mol) makes the proton–hydride combination proceed in a fashion similar to the protonation reactions in transition-metal hydrides rather than those in group 13 hydrides  $EH_4^-$  ( $E = B, Al, Ga$ ). As for the  $H_2$ -splitting reaction  $R_3BPR'_3 + H_2 \rightarrow [R_3BH^-][HPR'_3^+]$ , classical Lewis pair (CLP)  $(CF_3)_3BPH_3$  exhibits a high barrier and results in an unstable ion pair product  $[(CF_3)_3BH^-][HPH_3^+]$  compared with the “frustrated Lewis pair” (FLP)  $(C_6F_5)_3BP(tBu)_3$ . A detailed analysis of the mechanistic aspects of  $H_2$  activation by  $(CF_3)_3BPH_3$  and  $(C_6F_5)_3BP(tBu)_3$ , supported by another CLP  $(CF_3)_3BP(tBu)_3$  which has a binding energy comparable to  $(CF_3)_3BPH_3$  but a reaction exothermicity comparable to  $(C_6F_5)_3BP(tBu)_3$ , allows us to suggest that the low stability of FLP  $(C_6F_5)_3BP(tBu)_3$  is the determining factor for the low reaction barrier. The relative stability and other properties of the ion pair products  $[R_3BH^-][HPR'_3^+]$  have also been analyzed. Results strongly support the view proposed by Rokob et al. [Rokob, T. A.; Hamza, A.; Stirling, A.; Soos, T.; Papai, I. *Angew. Chem., Int. Ed.* **2008**, *47*, 2435] that the frustration energy lowers the energy barrier and increases the exothermicity of the reaction.

## Introduction

Hydrogen-bonding interactions are ubiquitous in chemical and biological systems and play a fundamental role not only in the molecular properties and structures but also in the chemical and biological processes. In general, hydrogen-bonding interactions fall into the category of weak interactions with a strength ranging from 2 to 10 kcal/mol.<sup>1</sup> However, this view has been challenged recently as more and more strong and unconventional hydrogen bonds have been recognized. Among them are the dihydrogen bonds (DHBs).<sup>2–7</sup> Like conventional hydrogen bonds, DHBs can influence structure, reactivity, and selectivity in the solution and solid states and have potential utilities in catalysis, crystal engineering, and materials chemistry. They also play an important role in proton-transfer processes.<sup>5,8</sup> The attractive bonding interactions in DHBs arise from the approaching of two oppositely charged hydrogen atoms and can be generally represented as a quartet  $X-H^{\delta+} \cdots H^{\delta-}-M$ , where X and M are more and less electronegative than hydrogen, respectively. While X is usually O or N, a typical element M that accommodates a hydridic hydrogen can be a transition metal and boron. This kind of proton–hydride ( $H^{\delta+} \cdots H^{\delta-}$ ) interac-

tion, mostly existing in transition-metal compounds, was identified in the middle of the 1990s and has been explored both experimentally and theoretically with several recent reviews focusing on this topic. The capability of main group element hydrides to form DHBs, however, was first elucidated by Crabtree<sup>3,9</sup> using aminoboranes. Richardson et al.’s<sup>3</sup> analysis of structures from the Cambridge Crystallographic Database (CSD) and spectroscopic studies showed that the N–H···H–B contact distances and heats of formation lie within the ranges of 1.7–2.2 Å (compared with the normal H···H contact of 2.4 Å) and 3–7 kcal/mol, respectively, comparable to conventional hydrogen bonds. During the past decade, the DHB concept has evolved via not only an elucidation of the bonding nature but also an extension of the range of hydrogen-bonding partners. The group 13 elements are known as electron-deficient atoms, and thus, much attention has been focused on their hydrides, which are better candidates to form DHBs than any other main group element hydrides,<sup>10–16</sup> though other hydride-bearing  $\sigma$ -bonds such as Li–H, Be–H, or even C(Si)–H<sup>7,14,17,18</sup> can also act as proton acceptors of DHBs. Most of these dihydrogen complexes have been theoretically studied with attempts to enrich our understanding of the nature of DHB interactions. Similar to the conventional hydrogen bonds, it is generally believed that the electrostatic proton–hydride attraction makes

\* To whom correspondence should be addressed. E-mail: weiwu@xmu.edu.cn (W.W.); yirong.mo@wmich.edu (Y.M.).

<sup>†</sup> Xiamen University.

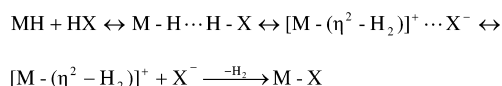
<sup>‡</sup> Western Michigan University.

a dominating contribution to the overall dihydrogen bonding energy, which depends on the nature of the acid and base subunits.

DHBs can be further classified either as a neutral pair, where both proton-donating and -accepting groups are neutral, or as a charge-assisted hydrogen bond (CAHB),<sup>19</sup> where a positive or negative charge on the proton-donating or -accepting group remarkably increases the strength of the hydrogen bond. Thus, strong and very strong DHBs are usually found in charged complexes. For example, DHBs with the BH<sub>4</sub><sup>−</sup> anion as the acceptor are stronger than those with neutral hydrides (e.g., BH<sub>3</sub>NEt<sub>3</sub> and BH<sub>3</sub>P(OEt)<sub>3</sub>) as acceptors, as demonstrated by experimental studies.<sup>10</sup> Comparably, MP2 calculations on the DHB complex of LiNCH<sup>+</sup>···HLi resulted in a much higher complexation energy (27.1 kcal/mol) than that of corresponding neutral pair NCH···HLi (8.8 kcal/mol).<sup>18</sup> Very strong DHBs such as NF<sub>3</sub>H<sup>+</sup>···HBeH, H<sub>2</sub>OH<sup>+</sup>···HBeBeH, or Cl<sub>2</sub>OH<sup>+</sup>···HBeH, with binding energies above 20 kcal/mol, also exhibit very short H···H intermolecular contacts (1.0–1.3 Å) and partial covalent nature.<sup>7,20</sup>

In general, however, the X–H<sup>δ+</sup>···<sup>δ−</sup>H–M species are unstable and tend to lose H<sub>2</sub>, leading to products with a new X–M bond.<sup>4</sup> In other words, dihydrogen-bonded species are transient intermediates when a hydride MH is approached by an acid XH. As such, proton transfer to hydridic hydrogen in DHBs with H<sub>2</sub> elimination and its reverse heterolytic splitting of H<sub>2</sub> have been the focus of a great deal of attention due to their key role in various chemical and biochemical processes.<sup>21</sup> This reversibility is of particular interest due to the potential of DHBs for the storage and production of hydrogen.<sup>22</sup> In fact, proton-transfer reactions involving transition-metal hydrides have been intensively studied in recent years.<sup>5,6,23</sup> It has been well established that the formation of a DHB complex X–H<sup>δ+</sup>···<sup>δ−</sup>H–M is the first stage in the protonation pathway of a transition-metal hydride. The subsequent proton transfer from the acidic X–H partner to the transition-metal hydride M–H, along the H···H bond, usually leads to the dihydrogen complex [M]η<sup>2</sup>–H<sub>2</sub>, which subsequently eliminates hydrogen upon heating (Scheme 1).

#### SCHEME 1



Compared with transition-metal hydrides, proton-transfer reactions involving main-group hydrides have been much less investigated. The elegant theoretical work of Filippov et al.<sup>13</sup> on proton-transfer and H<sub>2</sub>-elimination reactions of main-group hydrides EH<sub>4</sub><sup>−</sup> (E = B, Al, Ga) with alcohols showed not only the resemblance of DHB complexes of main-group and transition-metal hydrides but also the differences in the mechanistic aspects of the proton transfer in these systems, thus providing a better understanding of the trends in main-group hydride reactivity. Although the proton-transfer reactions of main-group hydrides behave much like those involving transition-metal hydrides in most respects, the very low stability of the main-group–(η<sup>2</sup>–H<sub>2</sub>) complexes due to their incapability of back-donation changes their role in proton-transfer reactions from intermediates to transition states. Other examples of the proton-transfer reactions of group 13 hydrides have also been reported, in particular, with H<sub>2</sub>O, HF, and HCl as proton donors.<sup>12</sup>

Significantly, Stephan and co-workers<sup>24,25</sup> recently introduced the concept of “frustrated Lewis pairs” (FLPs), in which

sterically hindered Lewis donors and acceptors are combined and their steric demands preclude them from forming simple Lewis acid–base adducts. They reported that H<sub>2</sub> can be readily activated at ambient temperature by FLPs R<sub>3</sub>BPR'<sub>3</sub> (R = C<sub>6</sub>F<sub>5</sub>; R' = *t*Bu, C<sub>6</sub>H<sub>2</sub>M<sub>3</sub>) by forming phosphonium borates of the form [R<sub>3</sub>PH][HR'<sub>3</sub>], R<sub>3</sub>BPR'<sub>3</sub> + H<sub>2</sub> → [R<sub>3</sub>BH<sup>−</sup>][HPR'<sub>3</sub><sup>+</sup>].<sup>25</sup> Subsequent theoretical studies suggested that the FLPs involve the preorganization of donor–acceptor sites into loosely bound but energetically strained complexes, which act as high reactive species for bond activation.<sup>26,27</sup> While the B–H···H–P interaction in ion pair molecule [R<sub>3</sub>BH<sup>−</sup>][HPR'<sub>3</sub><sup>+</sup>] primarily results from the oppositely charged (anion–cation) proton acceptor and donor, the dihydrogen bond is restrained compared to the above-mentioned neutral pairs or ion–molecule complexes. Apparently, such ion pair complexes are unstable due to a proton-transfer process leading to the H<sub>2</sub> formation, [R<sub>3</sub>BH<sup>−</sup>][HPR'<sub>3</sub><sup>+</sup>] → R<sub>3</sub>BPR'<sub>3</sub> + H<sub>2</sub>. Unique to the proton–hydride class of hydrogen bonds, such a proton transfer triggers the H<sub>2</sub> elimination. The role of ion pair complexes in H<sub>2</sub> release has been confirmed by computational studies of Nguyen et al.,<sup>28</sup> showing that the loss of H<sub>2</sub> from the ammonia borane dimer (BH<sub>3</sub>NH<sub>3</sub>)<sub>2</sub> can alternatively proceed via the ion pair isomer [BH<sub>4</sub><sup>−</sup>][NH<sub>3</sub>BH<sub>2</sub>NH<sub>3</sub><sup>+</sup>] with a lower energy barrier.

To further examine the role of substituted groups in R<sub>3</sub>BPR'<sub>3</sub> complexes and provide information for rational design and engineering of hydrogen storage materials, in this paper, we focused on the ion pair complexes [(CF<sub>3</sub>)<sub>3</sub>BH<sup>−</sup>][HPh<sub>3−*n*</sub>(Me)<sub>*n*</sub><sup>+</sup>] (*n* = 0–3) by performing computational studies to investigate the energetic, structural, electronic, and vibrational properties related to the dihydrogen bonding therein. Whereas the interaction nature within these ion pairs was probed by the block-localized wave function energy decomposition (BLW-ED) method,<sup>29–32</sup> the H<sub>2</sub>-activation/elimination process was also studied. In our preliminary calculations, the geometry optimizations of [(Me)<sub>3</sub>BH<sup>−</sup>][HPh<sub>3−*n*</sub>Me<sub>*n*</sub><sup>+</sup>] (*n* = 0–3) converged to B(Me)<sub>3</sub> + H<sub>2</sub> + Ph<sub>3−*n*</sub>(Me)<sub>*n*</sub> (*n* = 0–3), just like the case of H<sub>3</sub>B–H<sup>δ−</sup>···<sup>δ+</sup>H–NH<sub>3</sub>.<sup>33</sup> These initial results indicated that a spontaneous proton transfer occurs and the ion pairs [(Me)<sub>3</sub>BH<sup>−</sup>][HPh<sub>3−*n*</sub>Me<sub>*n*</sub><sup>+</sup>] are simply unstable in the gas phase. Subsequently, we replaced [B(CH<sub>3</sub>)<sub>3</sub>H<sup>−</sup>] with [B(CF<sub>3</sub>)<sub>3</sub>H<sup>−</sup>] as the proton acceptor, considering its weaker proton-accepting capability. As for proton donor [HPh<sub>3−*n*</sub>(Me)<sub>*n*</sub><sup>+</sup>] (*n* = 0–3), through chemical substitutions, their proton-donating ability can be altered gradually, and consequently, correlations among various properties of these complexes can be established and trends elucidated. We would like to point out that many efforts have been devoted, both from the experimental and theoretical points of view, to the rational design of hydrogen-bonded ion pair complexes in the gas phase.<sup>34</sup> Our results were presented in three main subsections. The first one concerned the analysis of the features of the B–H···H–P dihydrogen bonding in ion pair [(CF<sub>3</sub>)<sub>3</sub>BH<sup>−</sup>][HPh<sub>3−*n*</sub>(Me)<sub>*n*</sub><sup>+</sup>]. The second subsection dealt with the proton-transfer and H<sub>2</sub>-elimination reactions, [(CF<sub>3</sub>)<sub>3</sub>BH<sup>−</sup>][HPh<sub>3−*n*</sub>(Me)<sub>*n*</sub><sup>+</sup>] → (CF<sub>3</sub>)<sub>3</sub>B–Ph<sub>3−*n*</sub>(Me)<sub>*n*</sub> + H<sub>2</sub>. The last subsection centered on the H<sub>2</sub> activation by Lewis acid–base adducts reactions, R<sub>3</sub>BPR'<sub>3</sub> + H<sub>2</sub> → [R<sub>3</sub>BH<sup>−</sup>][HPR'<sub>3</sub><sup>+</sup>]. A comparison was made with the facile H<sub>2</sub>-splitting reaction by “frustrated Lewis pair” (C<sub>6</sub>F<sub>5</sub>)<sub>3</sub>BP(*t*Bu)<sub>3</sub>. Even though our model systems [(CF<sub>3</sub>)<sub>3</sub>BH<sup>−</sup>][HPh<sub>3−*n*</sub>(Me)<sub>*n*</sub><sup>+</sup>] (*n* = 0–3) have not been experimentally studied so far, theoretical investigations cannot only provide useful information on the structures and bonding of these complexes but also suggest future experiments.

## Methods Section

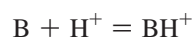
Structures of complexes  $[\text{B}(\text{CF}_3)_3\text{H}^-][\text{HPH}_{3-n}(\text{Me})_n^+]$  and all related monomers considered in this study have been optimized at the second-order Moller–Plesset perturbation theory (MP2) level with the 6-31++G(d,p) basis set. The minimum-energy nature of the optimized structures was verified from vibrational frequency analyses. The MP2/6-31++G(d,p) geometries were then adopted for single-point MP2/aug-cc-pVDZ calculations. The counterpoise method (CP) method was used to correct the basis set superposition errors (BSSE) in the calculation of the binding energy.<sup>35</sup> The natural population analysis (NPA) and the natural bond orbital (NBO) analysis<sup>36</sup> have been used to evaluate the atomic charges and the second-order interaction energies, respectively.

There are many theoretical approaches available to probe the nature of intermolecular interactions, often in terms of several physically meaningful components such as electrostatic, exchange, dispersion, relaxation or polarization, charge transfer, and so forth.<sup>30,37</sup> Among these energy decomposition schemes, the BLW-ED method has the advantage of defining the hypothetical electron-localized state self-consistently.<sup>29–32</sup> Moreover, the BLW has the geometry optimization capability and recently has been extended to the DFT level<sup>32,38</sup> and ported to the GAMESS software in our group.<sup>39</sup> Thus, both the structural and energetic changes due to the charge transfer among interacting species can be quantitatively evaluated. In this work, we performed the BLW-ED calculations at the DFT(B3LYP) level, which generally underestimates the dispersion effect. The latter can be well compensated by the electron-correlated MP2 method. As such, the binding energy  $\Delta E_b$  between  $[\text{B}(\text{CF}_3)_3\text{H}^-]$  (A) and  $[\text{HPH}_{3-n}(\text{Me})_n^+]$  (B) at the MP2 level can be well decomposed into the deformation energy  $\Delta E_{\text{def}}$ , Heitler–London energy  $\Delta E_{\text{HL}}$ , polarization energy  $\Delta E_{\text{pol}}$ , charge-transfer energy  $\Delta E_{\text{CT}}$ , and dispersion energy terms as

$$\begin{aligned}\Delta E_b(\text{MP2}) &= E(\text{AB};\text{MP2}) - E(\text{A};\text{MP2}) - E(\text{B};\text{MP2}) + \text{BSSE}(\text{MP2}) \\ &= E(\text{AB};\text{DFT}) - E(\text{A};\text{DFT}) - E(\text{B};\text{DFT}) + \text{BSSE}(\text{DFT}) + \Delta E_{\text{disp}} \\ &= \Delta E_{\text{def}} + \Delta E_{\text{HL}} + \Delta E_{\text{pol}} + \Delta E_{\text{CT}} + \Delta E_{\text{disp}}\end{aligned}$$

where the Heitler–London energy term is composed of both the electrostatic and Pauli repulsion interactions. We note that the recent energy decomposition scheme introduced by Khalullin et al.<sup>40</sup> under the name of “absolutely localized molecular orbitals” is identical to the BLW-ED approach.

Proton affinity (PA) is defined as a negative enthalpy of the following reaction



$$\text{PA}(\text{B}) = -\Delta H_{\text{rxn}}$$

Since the acidity of an acid A equals the proton affinity of the acid’s conjugate base,  $\text{A}^-$ , in this paper, we use the proton affinity (PA) of the conjugate base to represent the acidity of  $[\text{HPH}_{3-n}(\text{Me})_n^+]$ . G3(MP2)<sup>41</sup> theory has been employed to compute PAs. All calculations related to the geometry optimization, vibrational frequency analysis, and G3(MP2) theory have been carried out with the GAUSSIAN03 program using the

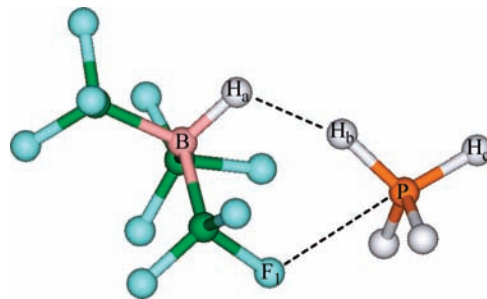


**Figure 1.** Optimized structure of complex  $[(\text{CF}_3)_3\text{BH}^-][\text{HPH}_3^+]$  at the MP2/6-31++G(d, p) level.

default Gaussian convergence criteria,<sup>42</sup> where the BLW-ED analyses have been performed with the GAMESS software.<sup>39</sup>

Due to the high computational demand for the MP2 energy scanning, the heterolytic hydrogen-splitting reactions,  $\text{R}_3\text{BPR}'_3 + \text{H}_2 \rightarrow [\text{R}_3\text{BH}^-][\text{HPR}'_3^+]$ , were explored at the B3LYP/6-31G(d) level with GAUSSIAN03, followed by single-point MP2/cc-pVTZ calculations<sup>43</sup> of key structures using the resolution-of-identity (RI) integral approximation. All of our RI-MP2/cc-pVTZ calculations were carried out with the program TURBOMOLE.<sup>44</sup> The electron density and its corresponding Laplacian at bond critical points were characterized using the AIM2000 program<sup>45</sup> based on Bader’s atoms in molecules (AIM) theory.<sup>46</sup>

## Results and Discussion

**1. The B–H···H–P Dihydrogen Bonding in Ion Pair Complexes.** The fully optimized ion pair complexes correspond to actual local minima on the potential energy surfaces. As an example, Figure 1 depicts the optimal structure of the complex  $[(\text{CF}_3)_3\text{BH}^-][\text{HPH}_3^+]$  at the MP2/6-31++G(d, p) level of theory. The rest of the ion pairs are of similar structures. The binding energies ( $\Delta E_b$ ) of ion pairs listed in Table 1 were calculated as the energy differences between fully optimized complexes and individually optimized monomers. Inclusion of the zero-point vibrational energies has very little effect on the binding energies. The magnitude of the basis set superposition error (BSSE), however, seems nontrivial, with a maximum value of 5.29 kcal/mol for complex **4**. It is interesting to note that the binding energy monotonously decreases from 82.40 in **1** to 73.24 kcal/mol in **4** with the gradual methyl substitutions. As well expected, the BLW-ED analyses (with data compiled in Table 2) confirmed that the binding within ion pair complexes  $[(\text{CF}_3)_3\text{BH}^-][\text{HPH}_{3-n}(\text{Me})_n^+]$  is dominated by the stabilizing electrostatic attraction, whereas the rest of the energy terms make limited contributions to the formation of ion pairs. Interestingly, the gradual substitution of methyl groups decreases the Heitler–London, polarization, and charge-transfer energy terms in the same trend of the overall binding energies. In contrast, the enlargement of the complex size from **1** to **4** increases the dispersion effect, albeit with a small magnitude.

As both the polarization and charge-transfer effects change the overall electron density of a complex, Figure 2 shows plots of the electron density difference (EDD) maps due to the polarization and charge-transfer interactions in complex **1**, where the red or blue color highlights the enhanced or reduced electron density, respectively. Apparently, the approach of the two reversely charged species disturbs the overall electron density and shifts electrons within  $[(\text{CF}_3)_3\text{BH}^-]$  to the  $[\text{HPH}_3^+]$  side. Unlike the polarization effect, charge transfer is more local and has impacts on interfacial atoms only. The electron transfer



**TABLE 1: Binding Energies and Reaction Energies (kcal/mol) for Ion Pair Complexes 1–4 at the MP2/aug-cc-pVDZ//MP2/6-31++G(d, p) Level**

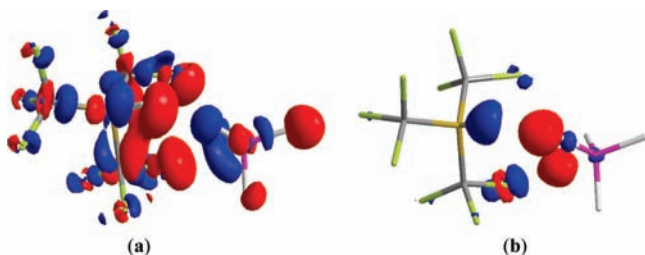
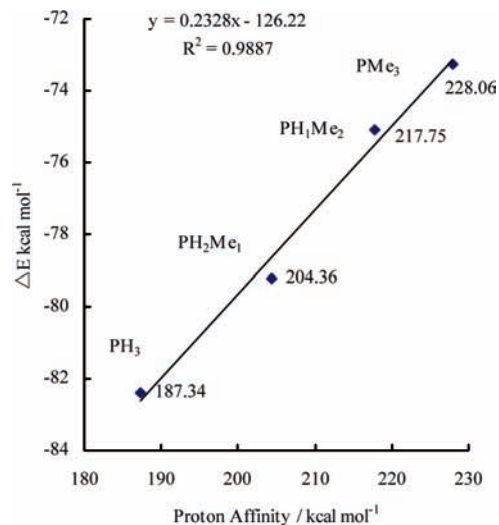
ion pair complexes	( $\Delta E_b$ )	( $\Delta E_b$ ) <sup>zpe, a</sup>	( $\Delta E_b$ ) <sup>zpe, cp b</sup>	$\Delta E_{pt}$ <sup>c</sup>	$\Delta E_r$ <sup>d</sup>
[(CF <sub>3</sub> ) <sub>3</sub> BH <sup>-</sup> ][HPH <sub>3</sub> <sup>+</sup> ] ( <b>1</b> )	-87.60	-85.74	-82.40	12.51	-27.31
[(CF <sub>3</sub> ) <sub>3</sub> BH <sup>-</sup> ][HPH(CH <sub>3</sub> ) <sub>2</sub> <sup>+</sup> ] ( <b>2</b> )	-84.77	-83.39	-79.21	26.05	-25.02
[(CF <sub>3</sub> ) <sub>3</sub> BH <sup>-</sup> ][HPH <sub>2</sub> (CH <sub>3</sub> ) <sub>1</sub> <sup>+</sup> ] ( <b>3</b> )	-80.84	-79.67	-75.08	34.78	-25.63
[(CF <sub>3</sub> ) <sub>3</sub> BH <sup>-</sup> ][HP(CH <sub>3</sub> ) <sub>3</sub> <sup>+</sup> ] ( <b>4</b> )	-79.64	-78.53	-73.24	43.34	-24.72

<sup>a</sup>  $\Delta E_B^{zpe}$  refers to binding energy after ZPE correction. <sup>b</sup>  $\Delta E_B^{zpe, cp}$  refers to binding energy after ZPE and BSSE corrections. <sup>c</sup> Reaction energy for [(CF<sub>3</sub>)<sub>3</sub>BH<sup>-</sup>][HPH<sub>3-n</sub>(Me)<sub>n</sub><sup>+</sup>] → B(CF<sub>3</sub>)<sub>3</sub>( $\eta^2$ -H<sub>2</sub>) + PH<sub>3-n</sub>(Me)<sub>n</sub>. <sup>d</sup> Reaction energy for [(CF<sub>3</sub>)<sub>3</sub>BH<sup>-</sup>][HPH<sub>3-n</sub>(Me)<sub>n</sub><sup>+</sup>] → B(CF<sub>3</sub>)<sub>3</sub>PH<sub>3-n</sub>(Me)<sub>n</sub> + H<sub>2</sub>.

**TABLE 2: Energy Contributions to the Binding Energies in Ion Pair Complexes 1–4 (kcal/mol) at the MP2/6-31++G(d, p) Level<sup>a</sup>**

energy term	1	2	3	4
deformation energy ( $\Delta E_{def}$ )	2.70	2.38	2.20	2.13
Heitler–London energy ( $\Delta E_{HL}$ )	-66.77	-65.09	-61.65	-60.11
polarization energy ( $\Delta E_{pol}$ )	-10.23	-8.79	-8.02	-7.38
charge-transfer energy ( $\Delta E_{ct}$ )	-6.86	-4.82	-4.11	-3.52
dispersion energy ( $\Delta E_{corr}$ )	-0.49	-1.84	-2.49	-3.32
binding energy ( $\Delta E_b$ )	-81.65	-78.16	-74.07	-72.20

<sup>a</sup> Structural parameters are based on the optimal geometries at the MP2/6-31++G(d, p) level.

**Figure 2.** Electron density difference (EDD) maps showing the electron density changes due to the effects of polarization [(a) with isodensity 0.002] and charge transfer [(b) with isodensity 0.001].**Figure 3.** Linear correlation between G3(MP2)-calculated proton affinities of the PH<sub>3-n</sub>Me<sub>n</sub> base and the binding energies of the ion pair complexes 1–4.

occurs from [(CF<sub>3</sub>)<sub>3</sub>BH<sup>-</sup>] to [HPH<sub>3</sub><sup>+</sup>] and measures the strength of covalence in hydrogen bonds.<sup>31</sup>

The correlations between energies and the PAs of the proton donors' conjugate bases have been discussed by many researchers for H bonds as well as for DHBs.<sup>47</sup> Figure 3 shows that the binding energies are in a good linear relationship with the acidity of proton donors.

Table 3 lists several selected geometrical parameters in the optimized ion pair complexes investigated in this study, along with the variations of the B–H<sub>a</sub> and P–H<sub>b</sub> bond distances upon complexation. In all cases, the H<sub>a</sub>···H<sub>b</sub> distances are shorter than the sum of their van der Waals radii (<2.4 Å), confirming the existence of an attractive interaction between B–H<sub>a</sub> and P–H<sub>b</sub> bonds. Reducing the proton-donor strength by successive methyl substitutions on the phosphorus atom of the PH<sub>4</sub><sup>+</sup> cation leads to the stretching of the H<sub>a</sub>···H<sub>b</sub> distance, which goes from 1.845 in **1** to 1.925 Å in **4**. In other words, the stronger the proton donor, the shorter the H<sub>a</sub>···H<sub>b</sub> distance. The B–H<sub>a</sub>···H<sub>b</sub> angles vary in the range of 109–114°, while the P–H<sub>a</sub>···H<sub>b</sub> angles remain near linear in the range of 158–169°, in agreement with results reported in the literature.<sup>10–13,16</sup> Previous studies<sup>10–13</sup> suggested that the formation of B–H<sup>δ-</sup>···<sup>δ+</sup>H–P would lead to the elongation of the proton-acceptor B–H<sub>a</sub> and proton-donor P–H<sub>b</sub> bond lengths compared with their values in isolated monomers. This seems true for the B–H<sub>a</sub> bond, which elongates about 0.005–0.007 Å. However, the changes in P–H<sub>b</sub> bond lengths seem random. Except in the case of **1**, the complexes **2–4** exhibit a slight shortening of the P–H<sub>b</sub> bond by 0.002–0.003 Å. This echoes the EDD maps in Figure 2 and indicates that the formation of ion pairs would demand noticeable electronic and structural reorganization accompanied by the strengthening of the proton-donating P–H<sub>b</sub> bond in some cases.

Upon DHB formation, a mutual polarization of the electron clouds of participating molecules should be expected, with a certain amount of electron density transferring from the proton-acceptor to the -donor molecule as in the cases of classical H bonds. The rearrangement of electron density will lead to the increase in the absolute value of both the positive charge on the acidic hydrogen and the negative charge on the proton-accepting atom. For the complexes studied in this work, the amount of overall charge transfer decreases from 0.0296 in **1** to 0.0175 e in **4**, as indicated in Table 4, in the order of decreasing proton-donating ability. As expected, the negative charge on the hydride atom and the positive charge on the hydrogen of the P–H<sub>b</sub> bond increase ( $\Delta q(H_a) = 0.022$ – $0.034$  e,  $\Delta q(H_b) = 0.019$ – $0.041$  e), and the amount of increasing charge again depends on the proton-donating capabilities. It is obvious from Table 4 that the stronger the proton donor, the more negative the hydridic H<sub>a</sub> atom and the more positive the protonic H<sub>b</sub> atom. Apart from the B–H<sub>a</sub>···H<sub>b</sub>–P DHB interaction, which is the biggest contributor to the ion pairs' stabilization, the NBO analysis indicated another significant stabilizing force from the negative hyperconjugation of lone pairs of the F<sub>1</sub> atom to the P–H<sub>c</sub> (or P–CH<sub>3</sub> in complexes **3** and **4**) antibonding orbital, which is similar to the case of ClCH<sub>3</sub>···FH, where electron transfer occurs from the lone pair on F to the remote antibonding  $\sigma^*(\text{CCl})$ .<sup>48</sup> As shown in Figure 1, the F<sub>1</sub>···P–H<sub>c</sub> angle is nearly linear and thus is favorable for the n(F<sub>1</sub>) →  $\sigma^*(\text{PH}_c)$  interaction.

**TABLE 3: Optimal Geometrical Parameters (Å for bond lengths and degrees for angles) for Ion Pair Complexes 1–4 at the MP2/6-31++G(d, p) Level**

complexes	$r(\text{H}_a\text{H}_b)$	$r(\text{BH}_a)$	$r(\text{PH}_b)$	$\angle\text{BH}_a\text{H}_b$	$\angle\text{PH}_b\text{H}_a$	$\Delta r(\text{BH}_a)$	$\Delta r(\text{PH}_b)$
<b>1</b>	1.845	1.210	1.389	113.0	159.0	0.007	0.004
<b>2</b>	1.903	1.209	1.387	111.9	158.4	0.006	−0.002
<b>3</b>	1.914	1.208	1.386	109.8	163.7	0.005	−0.002
<b>4</b>	1.925	1.208	1.387	109.1	168.3	0.005	−0.003

**TABLE 4: NBO Net Charges (e), Electron Densities  $\rho_c$  ( $\text{e} \text{Å}^{-3}$ ), and Laplacians  $\nabla^2\rho_c$  ( $\text{e} \text{Å}^{-5}$ ) at the  $\text{H}_a\cdots\text{H}_b$  Bond Critical Points<sup>a</sup>**

complexes	$q(\text{B})$	$q(\text{H}_a)$	$q(\text{H}_b)$	$q(\text{P})$	CT <sup>b</sup>	$\rho_c$	$\nabla^2\rho_c$
<b>1</b>	0.062 (0.067)	−0.065 (−0.031)	0.083 (0.064)	0.775 (0.743)	0.0296	0.0175	0.0463
<b>2</b>	0.065	−0.061	0.072 (0.041)	1.007 (0.984)	0.0202	0.0157	0.0435
<b>3</b>	0.066	−0.058	0.057 (0.021)	1.238 (1.225)	0.0195	0.0156	0.0434
<b>4</b>	0.066	−0.053	0.047 (0.006)	1.468 (1.463)	0.0175	0.0154	0.0430

<sup>a</sup> Calculated at the MP2/6-31++G(d, p) level. Monomer values are given in parentheses <sup>b</sup> Charge transferred (CT) from the proton acceptor (au).

Bader's AIM theory has been broadly applied to the elucidation of bonding natures in molecules.<sup>49</sup> The topological properties of the electronic charge density are derived to characterize the bonding pattern of complexes. The existence of a (3, −1) bond critical point (BCP) with a positive Laplacian usually corresponds to a noncovalent interaction. For all  $\text{H}_a\cdots\text{H}_b$  contacts in the present complexes **1–4**, the BCPs are of the (3, −1) type, with positive values for the Laplacian of the electron density (Table 4). The interactions are characterized as closed shells. The electron densities and their Laplacians at the BCPs range from 0.0154 to 0.0175 and 0.0430 to 0.0463, respectively, and are in the range acceptable for dihydrogen bonds.<sup>50</sup>

The blue-shifted or improper hydrogen bonds ( $\text{X}-\text{H}\cdots\text{Y}$ ), which exhibit changes (e.g., shortening of the  $\text{X}-\text{H}$  bond and blue shifting of the stretching frequency) opposite to those expected for normal hydrogen bonds, have received much experimental and theoretical attention.<sup>48,51,52</sup> However, studies of dihydrogen bonds in terms of frequency blue-shifting are scarce.<sup>53</sup> Alabugin et al. have shown that the  $\text{X}-\text{H}$  bond length in  $\text{X}-\text{H}\cdots\text{Y}$  hydrogen-bonded complexes is controlled by a balance of two main factors acting in opposite directions.<sup>52</sup> The “ $\text{X}-\text{H}$  bond lengthening” due to the  $n(\text{Y}) \rightarrow \sigma^*(\text{H}-\text{X})$  hyperconjugative interaction is offset by the “ $\text{X}-\text{H}$  bond shortening” due to the increase in the s character and polarization of the  $\text{X}-\text{H}$  bond. As mentioned above, the  $\text{P}-\text{H}_b$  bond for **2–4** is shortened by 0.002–0.003 Å upon complexation. While, in other cases, multiple H bonds are formed and both red- and blue-shifted hydrogen bonds can be observed, here, we investigate the complex **4** for the sake of simplicity. On the basis of the NBO analysis, the  $\sigma(\text{BH}_a) \rightarrow \sigma^*(\text{PH}_b)$  hyperconjugative energy seems nontrivial (4.9 kcal/mol).<sup>52</sup> However, the increase in  $\text{P}-\text{H}_b$  bond polarization and the decrease in effective electronegativity of the  $\text{H}_b$  atom upon the  $\text{B}-\text{H}_a\cdots\text{H}_b-\text{P}$  bond formation lead to an increase in the s character from 22.6 to 25.0% in the  $\text{P}-\text{H}_b$  bond, which is in excellent agreement with Bent's rule,<sup>54</sup> and subsequently the shortening of the  $\text{P}-\text{H}_b$  bond. A balance of these two effects results in a contraction of the  $\text{P}-\text{H}_b$  bond length in **4** by 0.003 Å, which is accompanied by a blue shift of its vibrational frequency by 9  $\text{cm}^{-1}$ .

**2. Proton-Transfer Reactions.** Proton-transfer (PT) reactions involving transition-metal hydrides with  $\text{H}_2$  loss have been well studied both experimentally and computationally, but little is known about the PT processes concerning main-group hydrides. The complexes addressed here differ from the earlier cases of group 13 hydrides in that the proton donors are positively charged with the proton acceptors negatively charged;

thus, overall, the complexes are neutral. The systems  $\text{EH}_4^-\cdots\text{HOR}(\text{HX})$  studied previously,<sup>12,13</sup> however, contain a net charge. It is worth mentioning that, on one hand, the  $[\text{HPH}_{3-n}(\text{CH}_3)_n]^+$  cation is more acidic than the neutral proton donor HOR or HX. The gas-phase acidities of HF and  $[\text{HP}(\text{CH}_3)_3]^+$ , for example, are calculated to be 372.7 and 187.3 kcal/mol, respectively, at the G3(MP2) level. On the other hand, differences between the proton acceptors  $[\text{B}(\text{CF}_3)_3\text{H}^-]$  and  $\text{EH}_4^-$  might show different proton-transfer mechanisms.

Unlike the PT process in  $\text{EH}_4^-\cdots\text{HOR}(\text{HX})$ , we were unable to locate a transition state (or saddle point) for the PT in ion pairs  $[(\text{CF}_3)_3\text{BH}^-][\text{HPH}_{3-n}(\text{Me})_n]^+$  due to the flatness of the energy profile around the barrier area. The potential energy profiles thus were computed by specifying the  $\text{H}_a\cdots\text{H}_b$  distance as the reaction coordinate with all of the rest of the degrees of freedom optimized at the MP2/6-31++G(d,p) level, except for the largest system  $[(\text{CF}_3)_3\text{BH}^-][\text{HP}(\text{CH}_3)_3]^+$  (**4**) for which the energy profile scanning proved to be computationally demanding. Instead, we used the B3LYP/6-311++G(d,p) level for **4**. Figure 4 shows the minimum-energy profiles along the proton-transfer pathway in the four systems, where the total energy changes  $\Delta E$  relative to the isolated monomers  $\text{B}(\text{CF}_3)_3(\eta^2-\text{H}_2)$  and  $\text{PH}_{3-n}(\text{Me})_n$  were plotted as a function of the  $\text{H}_a\cdots\text{H}_b$  distance. Figure 4 shows that the proton-transfer processes correspond to single-well potentials. At long proton–hydride distances ( $>1.6$  Å), the PESs appear to be very flat, showing the structural flexibility of the ion pairs. Complex  $[(\text{CF}_3)_3\text{BH}^-][\text{HPH}_{3-n}(\text{Me})_n]^+$  is initially formed as a minimum in the protonation pathway. The energy of the system increases steadily as the proton departs from the parent  $[\text{HPH}_{3-n}(\text{Me})_n]^+$  subunit to the  $[\text{B}(\text{CF}_3)_3\text{H}^-]$  acceptor, leading to the direct formation of the dihydrogen complex  $(\text{CF}_3)_3\text{B}(\eta^2-\text{H}_2)$ . In the case of **1**, however, an intermediate  $\text{B}(\text{CF}_3)_3(\eta^2-\text{H}_2)\cdots\text{PH}_3$  (**IM<sub>CLP</sub>**), as shown in Figure 5, can be identified. To our knowledge, this is the first time when such an intermediate in the proton-transfer pathway between the main-group ( $\eta^2-\text{H}_2$ ) and neutral molecule has been generated. For other cases (**2–4**), no energy minima like **IM<sub>CLP</sub>** have been located, and all attempts to generate such kinds of structures have ended up in the initial ionic pairs  $[(\text{CF}_3)_3\text{BH}^-][\text{HPH}_{3-n}(\text{Me})_n]^+$ , which is similar to a previous study of the protonation of the transition-metal hydrides.<sup>23</sup>

Transition-metal dihydrogen complexes have H–H distances ranging from 0.8 to 1.0 Å, and hundreds of these complexes have been reported as isolable species.<sup>5,6,23,55</sup> The bonding interactions between a metal complex and hydrogen have been

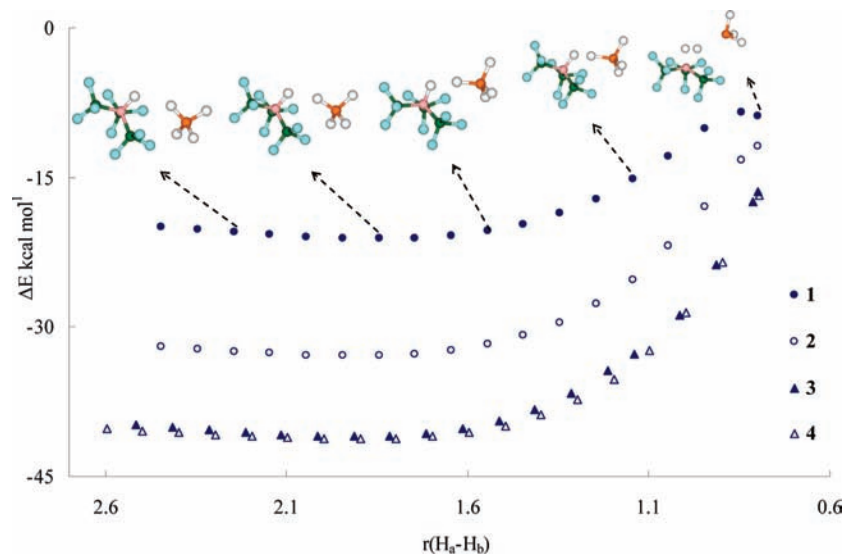


**Figure 4.** Potential energy curves corresponding to the proton transfer within ion pair complexes  $[(CF_3)_3BH^-][HPH_{3-n}(CH_3)_n^+]$  ( $n = 0-3$ ) derived at the MP2/6-31++G(d,p) and B3LYP/6-311++G(d,p) levels for **1-3** and **4**, respectively. The total energy of the optimized isolated monomers  $B(CF_3)_3(\eta^2-H_2)$  and  $PH_{3-n}(CH_3)_n$  is set as 0 for each curve.

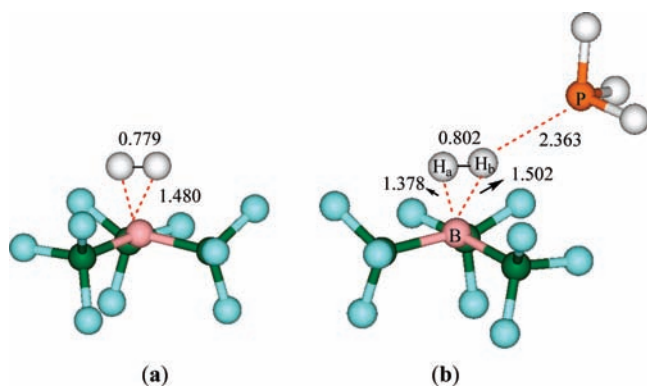


**Figure 5.** Optimized structures of dihydrogen complex  $B(CF_3)_3(\eta^2-H_2)$  (a) and the intermediate  $B(CF_3)_3(\eta^2-H_2)\cdots PH_3$  (b) at the MP2/6-31++G(d,p) level.

described in terms of donation from the filled  $\sigma_{H-H}$  bonding orbital into an empty orbital of  $\sigma$  symmetry on the metal. This interaction is augmented by the back-donation from the filled metal orbitals of predominant d character to the  $\sigma^*$  orbital of  $H_2$ . Both of these interactions weaken and lengthen the H–H bond. Because of the nonexistence of combined forward- and back-donations, contrarily to what happens with transition-metal hydrides, for main-group hydrides, the dihydrogen complexes are generally not stable. Though the  $BH_3(\eta^2-H_2)$  complex has been experimentally detected (IR spectra in a cryogenic matrix at 13–27 K),<sup>56</sup> its binding energy has been calculated to be only 1.5 kcal/mol.<sup>57</sup> In fact, the  $BH_5$  complex has been the subject of numerous high-level quantum mechanical studies.<sup>57–59</sup> Our MP2/6-31++G(d, p) optimization also indicated that the  $B(CF_3)_3(\eta^2-H_2)$  complex is a minimum (Figure 5). More accurate MP2/aug-cc-pVDZ calculation showed the H–H distance of 0.795 Å and  $D_0/D_0 = 10.8/6.0$  kcal/mol for the dissociation of  $B(CF_3)_3(\eta^2-H_2)$  to  $B(CF_3)_3$  and  $H_2$ , which is higher than that of  $BH_3(\eta^2-H_2)$  ( $D_0/D_0 = 6.6/1.2$  kcal/mol).<sup>59</sup> These results indicate that  $B(CF_3)_3(\eta^2-H_2)$  is more stable than  $BH_3(\eta^2-H_2)$ . The substitutions of H atoms of  $BH_3$  by the more electronegative  $CF_3$  groups increase the electron-accepting capability of the vacant 2p orbital on boron from a base. Another reason for the stability of  $B(CF_3)_3(\eta^2-H_2)$  is the back-donation from the filled 2p orbitals of F atoms of the  $CF_3$  groups to the  $\sigma^*$  orbital of  $H_2$

based on the NBO analysis, which is comparable to the  $d(M) \rightarrow \sigma^*(H_2)$  back-donation for transition-metal dihydrogen complexes. However, the present complex  $B(CF_3)_3(\eta^2-H_2)$  is still less stable than most metal– $H_2$  complexes.

As suggested by Filippov et al.,<sup>13</sup> the limited stability of the main-group– $(\eta^2-H_2)$  complexes may affect the proton-transfer mechanism. The higher stability of  $B(CF_3)_3(\eta^2-H_2)$  compared to that of  $BH_3(\eta^2-H_2)$  makes the proton-transfer reactions between  $[B(CF_3)_3H^-]$  and  $[HPH_{3-n}(Me)_n^+]$  take place with a mechanism somewhat similar to that reported for transition-metal hydride protonations as no saddle points can be found for these proton-transfer reactions. The first step transforms the ion pair  $[B(CF_3)_3H^-][HPH_{3-n}(Me)_n^+]$  to a complex of neutral molecules  $B(CF_3)_3(\eta^2-H_2)$  and  $PH_{3-n}(CH_3)_n$ . This step is unfavorable, but the reaction barrier should be lower than the value of  $\Delta E_{pt}$  (see Table 1) due to the  $B(CF_3)_3(\eta^2-H_2)\cdots PH_{3-n}(CH_3)_n$  interaction. For instance, the intermediate  $IM_{CLP}$  is stabilized by 6.0 kcal/mol upon the complexation between  $B(CF_3)_3(\eta^2-H_2)$  and  $PH_3$  at the MP2/aug-cc-pVDZ//MP2/6-31++G(d, p) level. The values of  $\Delta E_{pt}$  indicate that the reaction barrier decreases with more acidic proton donors and is lower in most cases than the reaction barrier of  $BH_4^- + HOR$  with reference to  $BH_4^-\cdots HOR$  as the zero point in the energy profile. The proton-transfer process is followed by the next step corresponding to the  $H_2$  elimination to yield the Lewis acid–base adduct  $(CF_3)_3BPH_{3-n}(CH_3)_n$  and  $H_2$ . This step is strongly exothermic for all systems (the last column of Table 1), ranging from –24.72 to –27.31 kcal/mol, depending on the proton-donation strengths.

**3. The Heterolytic Cleavage of  $H_2$  by Lewis Pairs.** The heterolytic activation of  $H_2$  is a common reaction pathway that allows  $H_2$  to be effectively cleaved into  $H^+$  and  $H^-$  and thus is a crucial step to many biological and industrial processes utilizing  $H_2$  as a feedstock. Obviously, heterolytic  $H_2$  activation can be regarded as the reverse process of proton-transfer reactions discussed above,  $(CF_3)_3BPH_{3-n}(CH_3)_n + H_2 \rightarrow [(CF_3)_3BH^-][HPH_{3-n}(Me)_n^+]$ . By comparison with the facile heterolytic cleavage of dihydrogen by FLP,<sup>25,26</sup> we could get a better understanding of this type of reaction. As such, we considered the  $H_2$  activation by the classical Lewis pair (CLP)  $(CF_3)_3BPH_3$ , which is the final product of the proton-transfer



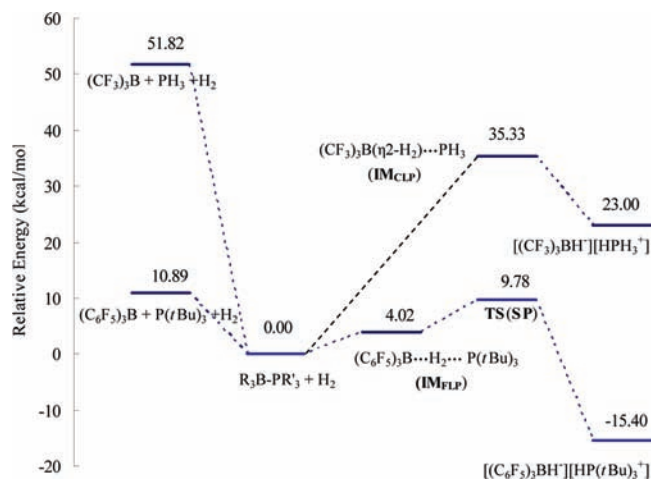


**Figure 6.** Potential energy profiles for the heterolytic cleavage of  $\text{H}_2$  by the classical Lewis pair  $\text{B}(\text{CF}_3)_3\text{PH}_3$  and the “frustrated Lewis pair”  $(\text{C}_6\text{F}_5)_3\text{BP}(\text{tBu})_3$  calculated at the MP2/6-31++G(d,p) and SCS-RIMP2/cc-pVTZ//B3LYP/6-31G(d) levels, respectively. The data related to FLP are taken from ref 26.

reaction in **1**, and the FLP  $(\text{C}_6\text{F}_5)_3\text{BP}(\text{tBu})_3$ , which has been both experimentally and theoretically investigated.<sup>25,26</sup> For the purpose of comparison, we also investigated the reactions of  $\text{H}_2$  with  $(\text{CF}_3)_3\text{BP}(\text{tBu})_3$  and  $(\text{C}_6\text{F}_5)_3\text{BPH}_3$  obtained by exchanging the Lewis acid or base subunit between  $(\text{CF}_3)_3\text{BPH}_3$  and  $(\text{C}_6\text{F}_5)_3\text{BP}(\text{tBu})_3$ . Unless otherwise specified, the geometries and energies related to  $(\text{C}_6\text{F}_5)_3\text{BP}(\text{tBu})_3$  are taken from ref 26. For complexes related to  $(\text{CF}_3)_3\text{BP}(\text{tBu})_3$  and  $(\text{C}_6\text{F}_5)_3\text{BPH}_3$ , calculations were carried out at the RI-MP2/cc-pVTZ//B3LYP/6-31G(d) level of theory. Figure 6 presented the relative energies associated with the heterolytic cleavage of  $\text{H}_2$  by  $(\text{CF}_3)_3\text{BPH}_3$  and  $(\text{C}_6\text{F}_5)_3\text{BP}(\text{tBu})_3$ , with the total energy of separated  $\text{R}_3\text{BPR}'_3$  and  $\text{H}_2$  set as a zero point.

Upon the interaction with the lone pair of  $\text{PH}_3$ , the  $\text{H}_a\text{—H}_b$  distance of  $\text{IM}_{\text{CLP}}$  is lengthened by 0.003 Å as compared to that for the isolated molecule (Figure 5), accompanied by the shortening of the  $\text{B—H}_a$  distance and the elongation of the  $\text{B—H}_b$  distance. The NPA charges [ $q(\text{H}_a) = 0.145$ ,  $q(\text{H}_b) = 0.260$ ] indicate the net loss of electrons and the polarization of electron density in  $\text{H}_2$ . However, the structural arrangement of  $\text{IM}_{\text{CLP}}$  seems in favor of the electron transfer through  $\text{H}_3\text{P} \rightarrow \sigma^*(\text{H}_2)$  and  $\sigma(\text{H}_2) \rightarrow \text{B}(\text{CF}_3)_3$  donations in a push–pull manner. These electronic properties described above are consistent with those suggested by Rokob et al. for  $\text{H}_2$  cleavage by FLP  $(\text{C}_6\text{F}_5)_3\text{BP}(\text{tBu})_3$ .<sup>26</sup> Figure 7 shows the variations of structural parameters and electronic properties along the  $\text{H}_2$ -splitting process,  $\text{B}(\text{CF}_3)_3(\eta^2\text{-H}_2)\cdots\text{PH}_3 \rightarrow [(\text{CF}_3)_3\text{BH}^-][\text{HPH}_3^+]$ . The change of the sign of the Laplacian value is first observed between atoms P and  $\text{H}_b$  in the structure with  $r(\text{H}_a\text{H}_b) = 0.945$  Å. The negative Laplacian indicates the partially covalent nature of such a connection in this structure, which explains a sharp decrease in the bond distance of  $\text{P—H}_b$  and a sudden change in  $q(\text{H}_a)$ . Upon the interaction between P and  $\text{H}_b$  atoms and the enhanced polarization effect, the  $\text{H}_a\text{—H}_b$  bond breaks heterolytically in the structure with  $r(\text{H}_a\text{H}_b) = 1.145$  Å on the basis of the positive Laplacian. In contrast to the  $\text{P—H}_b$  and  $\text{H}_a\text{—H}_b$  bonds, the formation of the  $\text{B—H}_a$  bond is slow, and its bond distance changes very smoothly. Along the entire  $\text{H}_2$ -splitting process, the electron densities at the  $\text{B—H}_a$  and  $\text{P—H}_b$  bond critical points increase steadily, but the density at the bond critical point of  $\text{H}_a\text{—H}_b$  decreases. The potential energy curve **1** of Figure 4 shows a negligible barrier of 0.32 kcal/mol for the  $\text{H—H}$  activation from  $\text{IM}_{\text{CLP}}$ .

In the case of FLP, an intermediate  $(\text{C}_6\text{F}_5)_3\text{B}\cdots\text{H}_2\cdots\text{P}(\text{tBu})_3$  ( $\text{IM}_{\text{FLP}}$ ) is initially formed (Figure 6), and the reaction proceeds via a saddle point (**SP**, often approximated as a transition state) which lies about 9.78 kcal/mol in energy above  $(\text{C}_6\text{F}_5)_3\text{BP}(\text{tBu})_3 + \text{H}_2$ .  $\text{IM}_{\text{CLP}}$  (CLP) and **SP** (FLP) represent the highest stationary points along the CLP and FLP reaction pathways, respectively, and the  $\text{H—H}$  distances in these states are very similar (i.e., 0.802 and 0.793 Å, respectively). We note that previous studies focused on the  $\text{R}_3\text{B}\cdots\text{H}_2$  and  $\text{R}'_3\text{P}\cdots\text{H}_2$  interactions and the role of “frustration” for the reactivity of FLPs.<sup>25,26</sup> By comparing with the reactions of  $(\text{CF}_3)_3\text{BPH}_3$  and  $(\text{CF}_3)_3\text{BP}(\text{tBu})_3$  with  $\text{H}_2$ , here, we provided some additional insights to the study. We considered three types of two-body interactions including  $\text{R}_3\text{B}\cdots\text{PR}'_3$ ,  $\text{R}_3\text{B}\cdots\text{H}_2$ , and  $\text{R}'_3\text{P}\cdots\text{H}_2$  (denoted with  $\text{X}\cdots\text{Y}$  in general) and their influence on the energy barriers for both reaction pathways. Table 5 compiled the relative energies of the fragment  $\text{X}\cdots\text{Y}$  with the geometries identical to that observed in  $\text{IM}_{\text{CLP}}$  and **SP**. As can be seen, the interactions between  $\text{R}'_3\text{P}$  and  $\text{H}_2$  are repulsive due to the Pauli exchange interaction in both  $\text{IM}_{\text{CLP}}$  and **SP**. Essentially the repulsive energies in both structures are the same. The second column of Table 5, consistent with what we discussed above, indicates the stability of  $\text{B}(\text{CF}_3)_3(\eta^2\text{-H}_2)$ . In contrast to the existence of a potential energy minimum in the case of  $\text{B}(\text{CF}_3)_3$ , the access of  $\text{H}_2$  to  $\text{B}(\text{C}_6\text{F}_5)_3$  is unfavorable, owing to the Pauli repulsion.<sup>26</sup> These results indicate that both of the interactions of  $\text{H}_2$  with  $\text{BR}_3$  and  $\text{PR}'_3$  suggested previously<sup>25</sup> are not favorable for the reactivity of FLP. While the formation of the intermediate  $\text{IM}_{\text{CLP}}$  requires the cleavage of the classical donor–acceptor bond between  $\text{B}(\text{CF}_3)_3$  and  $\text{PH}_3$ , which proves to be energetically demanding, the energetic cost is only 6.38 kcal/mol for the  $\text{B}(\text{CF}_3)_3\text{B}\cdots\text{P}(\text{tBu})_3$  part moving from the equilibrium geometry to the structure in **SP**. “The frustration energy”,<sup>26</sup> defined as the difference between the binding energies of the two types of Lewis pairs, reaches 40.9 kcal/mol (Figure 6). As such, only the structural flexibility and weak interaction within  $\text{B}(\text{CF}_3)_3\text{B}\cdots\text{P}(\text{tBu})_3$  would be favorable for the formation of **SP**. We note that the  $\text{H}_2$  molecule is more polarized in **SP** than in  $\text{IM}_{\text{CLP}}$ . Despite this, it appears that the electronic effect is not responsible for the reactivity of FLPs. This is supported by the calculations of the  $\text{H}_2$  activation by CLP  $(\text{CF}_3)_3\text{BP}(\text{tBu})_3$ . The reaction energies of  $\text{R}_3\text{BPR}'_3 + \text{H}_2 \rightarrow [\text{R}_3\text{BH}^-][\text{HPR}'_3^+]$  for  $(\text{C}_6\text{F}_5)_3\text{BP}(\text{tBu})_3$  and  $(\text{CF}_3)_3\text{BP}(\text{tBu})_3$  are very close (−15.4 and −13.8 kcal/mol, respectively). Optimization of the structure of  $\text{B}(\text{CF}_3)_3(\eta^2\text{-H}_2)\cdots\text{P}(\text{tBu})_3$ , like  $\text{IM}_{\text{CLP}}$  with a  $\text{P—H}_b$  distance of 3.9 Å, larger than that in  $\text{IM}_{\text{FLP}}$  (3.4 Å) of FLP reaction pathway, ends up with the final product  $[\text{B}(\text{CF}_3)_3\text{H}^-][\text{HP}(\text{tBu})_3^+]$ . This indicates that when the Lewis acid and base of  $(\text{CF}_3)_3\text{BP}(\text{tBu})_3$  are separated to some extent, it can split  $\text{H}_2$  in a more easy way. Nevertheless, the binding energy of 43.7 kcal/mol for  $(\text{CF}_3)_3\text{BP}(\text{tBu})_3$  would limit its reactivity for the  $\text{H}_2$  activation, similar to the experimental observations of no reaction for some CLPs such as  $\text{B}(\text{C}_6\text{F}_5)_3\text{P}(\text{Me})_3$  with  $\text{H}_2$  under mild conditions. Again, the primary reason for the low energy barrier of FLPs is their weak association and structural flexibility.

Another point worthy of our consideration is the relative stability of the ion pair  $[\text{R}_3\text{BH}^-][\text{HPR}'_3^+]$  with respect to  $\text{R}_3\text{BPR}'_3 + \text{H}_2$ . As can be seen from Figure 6, the ion pair  $[(\text{CF}_3)_3\text{BH}^-][\text{HPH}_3^+]$  lies 23.0 kcal/mol above  $(\text{CF}_3)_3\text{BPH}_3 + \text{H}_2$ , whereas the counterpart for FLP is favored by 15.4 kcal/mol over the neutral starting reactant. The last column of Table 1 indicates the instability of **2–4**, as in the case of **1**. In the extreme situation, as noted in the Introduction, a spontaneous

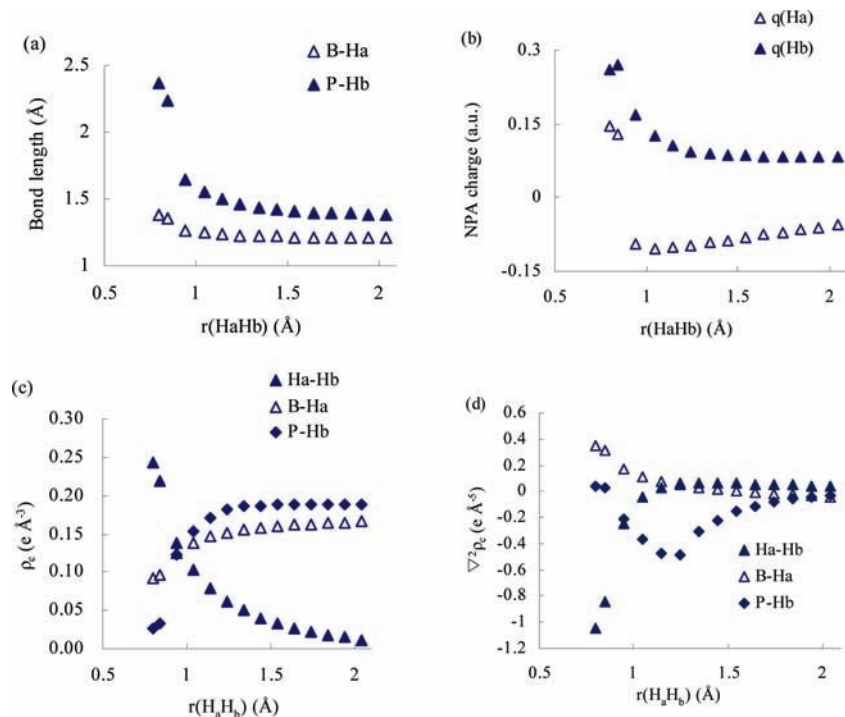


**Figure 7.** Changes in (a) the B–H<sub>a</sub> and P–H<sub>b</sub> distance, (b) the NPA charges of the H<sub>a</sub> and H<sub>b</sub> atoms, (c) the electron density of the bond critical points for the H<sub>a</sub>–H<sub>b</sub>, B–H<sub>a</sub>, and P–H<sub>b</sub> bonds, and (d) the Laplacian of the electron density at the bond critical point along the H<sub>a</sub>–H<sub>b</sub> bond-splitting process,  $\text{B}(\text{CF}_3)_3(\eta^2\text{-H}_2)\cdots\text{PH}_3 \rightarrow [(\text{CF}_3)_3\text{BH}^-][\text{HPH}_3^+]$  (**1**) with respect to the  $r(\text{H}_a\text{H}_b)$  distance. The structures for analysis here are taken from **1** of Figure 4.

**TABLE 5: Relative Energies (kcal/mol) of Fragment X···Y with Geometry Identical to Those Observed in IM<sub>CLP</sub> and TS(SP), Calculated at the MP2/61-31++G(d,p) and RI-MP2/cc-pVTZ//B3LYP/6-31G(d) Levels, respectively**

	$\text{R}'_3\text{P}\cdots\text{H}_2^a$	$\text{R}_3\text{B}\cdots\text{H}_2^b$	$\text{R}_3\text{B}\cdots\text{PR}'_3^c$
IM <sub>CLP</sub>	7.74	−6.32	55.70
TS(SP)	7.82	10.03	6.38

<sup>a</sup> Relative to  $\text{R}'_3\text{P} + \text{H}_2$ . <sup>b</sup> Relative to  $\text{R}_3\text{B} + \text{H}_2$ . <sup>c</sup> Relative to the equilibrium geometry of  $\text{R}_3\text{B}–\text{PR}'_3$ .

**TABLE 6: The Separate Reaction Energies  $\Delta E$  (kcal/mol) for the Heterolytic Activation of H<sub>2</sub> by Lewis Pairs,  $\text{R}_3\text{BP}'_3 + \text{H}_2 \rightarrow [\text{R}_3\text{BH}^-][\text{HPR}'_3^+]$**

separate reactions	$(\text{CF}_3)_3\text{BPH}_3^a$	$(\text{C}_6\text{F}_5)_3\text{BP}(t\text{Bu})_3^b$
$\text{H}_2 \rightarrow \text{H}^+ + \text{H}^-$	410.48	425.11
$\text{R}_3\text{B}–\text{PR}'_3 \rightarrow \text{R}_3\text{B} + \text{PR}'_3$	51.82	10.89 <sup>c</sup>
$\text{R}_3\text{B} + \text{H}^- \rightarrow \text{R}_3\text{BH}^-$	−156.93	−132.32
$\text{PR}'_3 + \text{H}^+ \rightarrow \text{HPR}'_3^+$	−197.42	−250.79
$\text{R}_3\text{BH}^- + \text{HPR}'_3^+ \rightarrow [\text{R}_3\text{BH}^-][\text{HPR}'_3^+]$	−84.94	−68.29 <sup>c</sup>
$\text{R}_3\text{B}–\text{PR}'_3 + \text{H}_2 \rightarrow [\text{R}_3\text{BH}^-][\text{HPR}'_3^+]$	23.01	−15.40

<sup>a</sup> Calculated at the MP2/6-31++G(d, p)//MP2/6-31++G(d, p) level. <sup>b</sup> Calculated at the RI-MP2/cc-pVTZ//B3LYP/6-31G(d) level. <sup>c</sup> Reference 26.

proton transfer from  $[\text{HPR}'_3^+]$  toward  $[\text{R}_3\text{BH}^-]$  can be observed. Any ion pair product of low stability is not suitable for H<sub>2</sub> storage as the strongly exothermic nature of the reaction is likely to prevent the use of these systems for the reversible dihydrogen activation. The understanding of the stability of ion pairs here is critical to the rational design of H<sub>2</sub> storage materials. Here, we provided a simple way to understand the reaction energy of  $\text{R}_3\text{BP}'_3 + \text{H}_2 \rightarrow [\text{R}_3\text{BH}^-][\text{HPR}'_3^+]$  in the cycle of several steps. These separated reactions, together with values of  $\Delta E$ , are compiled in Table 6. The first two steps are unfavorable for the stability of ion pair  $[\text{R}_3\text{BH}^-][\text{HPR}'_3^+]$ , and the other three are favorable. The implications of these data are clear. By com-

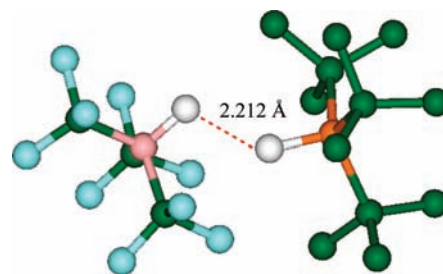


**Figure 8.** Optimized structure of the ion pair  $[(\text{CF}_3)_3\text{BH}^-][\text{HP}(t\text{Bu})_3^+]$  at the B3LYP/6-31G(d) level. The hydrogen atoms of the CH<sub>3</sub> group are omitted for clarity.

parison with the case of CLP, the major contributing factors to the stability of ion pair  $[(\text{C}_6\text{F}_5)_3\text{BH}^-][\text{HP}(t\text{Bu})_3^+]$  are the low binding energy and the high protonation energy or proton affinity of  $\text{P}(t\text{Bu})_3$ . The proton affinity gives a measure of the basicity of the molecule. The computed values for  $\text{PH}_3$  and  $\text{P}(t\text{Bu})_3$  are 197.4 and 250.8 kcal/mol, respectively, in good accord with the knowledge that due to the electron-donating capability, alkyl groups stabilize the adjacent positively charged atom and thus increase the basicity of the substance. The larger proton affinity of the substituted bases stabilizes the classical hydrogen-bonded  $\text{A}^-\cdots\text{H}–\text{B}^+$ , as shown by Alavi et al.<sup>33</sup> The Lewis acid  $\text{B}(\text{CF}_3)_3$  of CLP, however, stabilizes an ion pair much more than  $\text{B}(\text{C}_6\text{F}_5)_3$  does, as can be garnered from the reaction energies of  $\text{R}_3\text{B} + \text{H}^- \rightarrow \text{R}_3\text{BH}^-$ . In addition, the attractive Coulombic interaction between  $[\text{R}_3\text{BH}^-]$  and  $[\text{HPR}'_3^+]$  does not differ too much from the others and plays a minor role in the differentiation of  $[(\text{CF}_3)_3\text{BH}^-][\text{HPH}_3^+]$  and  $[(\text{C}_6\text{F}_5)_3\text{BH}^-][\text{HP}(t\text{Bu})_3^+]$ . The optimized structure of ion pair  $[(\text{CF}_3)_3\text{BH}^-][\text{HP}(t\text{Bu})_3^+]$  related to  $(\text{CF}_3)_3\text{BP}(t\text{Bu})_3$  is shown in Figure 8. This structure corresponds to a potential energy minimum and, as we mentioned above, is more stable than  $(\text{CF}_3)_3\text{BP}(t\text{Bu})_3 + \text{H}_2$  by −13.8 kcal/mol, despite the binding energy of 43.7 kcal/mol for  $(\text{CF}_3)_3\text{BP}(t\text{Bu})_3$ .



As far as  $[(C_6F_5)_3BH^-][HPH_3^+]$  is concerned, the calculation ends up with  $B(C_6F_5)_3 + H_2 + PH_3$ . These results are in accord with what we discussed above.

The heterolytic cleavage of dihydrogen by CLP is characterized by the high barrier and the instability of ion pair  $[R_3BH^-][HPR'_3^+]$ . Both characteristics are related to the strong binding within the Lewis acid–base complex  $(CF_3)_3BPH_3$ . The frustration energy (40.9 kcal/mol) lowers the activation barrier and increases the exothermicity of the reaction  $(C_6F_5)_3BP(tBu)_3 + H_2$ , in full agreement with what was suggested previously.<sup>26</sup> The main driving force for the  $H_2$  activation by FLP is the exothermicity of the reaction  $R_3BPR'_3 + H_2 \rightarrow [R_3BH^-][HPR'_3^+]$ .

## Conclusion

Theoretical studies of the  $B-H\cdots H-P$  dihydrogen bonding in ion pair complexes  $[(CF_3)_3BH^-][HPH_{3-n}(Me)_n^+]$  ( $n = 0-3$ ) and its role in the proton transfer with the  $H_2$  loss and the  $H_2$  activation by Lewis acid–base adducts have been carried out using quantum mechanical MP2 and DFT methods. The ion pair interaction energies are linearly dependent on the gas-phase acidity of the proton donor  $[HPH_{3-n}(Me)_n^+]$ , and the  $B-H\cdots H-P$  dihydrogen bonds account for most of their strength. The linear configuration of the  $H\cdots H-P$  moieties, the propensity for the proton transfer and the rearrangement of electron densities, and the topological properties of the DHB critical point for  $B-H\cdots H-P$  interactions studied herein are similar to those previously reported for neutral pairs and ion–molecule complexes. However, the formation of ion pairs causes significant electronic and structural reorganization, and there are several interactions contributing to the overall stabilization of ion pairs. As such, the shortening of the  $P-H$  bond in the proton donor  $[HPH_{3-n}(Me)_n^+]$  accompanied by a blue-shifting of its vibrational frequency in complexes **2–4** can be observed.

Due to the higher stability of the dihydrogen complex  $B(CF_3)_3(\eta^2-H_2)$ , the proton transfer within  $[(CF_3)_3BH^-][HPH_{3-n}(Me)_n^+]$  leads to the direct formation of the dihydrogen complex  $B(CF_3)_3(\eta^2-H_2)$  followed by  $H_2$  release. The higher stability of  $B(CF_3)_3(\eta^2-H_2)$  makes the PT reactions proceed in a different mechanism compared to those previously reported for group 13 hydrides  $EH_4^-$  ( $E = B, Al, Ga$ ). A more acidic proton donor  $[HPH_{3-n}(Me)_n^+]$  further lowers the reaction barrier in the process.

Two points should be emphasized on the heterolytic activation of  $H_2$  by Lewis pairs. One is the relative stability of the ion pair  $[R_3BH^-][HPR'_3^+]$  with respect to the reactants. Increasing the acidity of  $R_3B$  and basicity of  $PR'_3$  and decreasing the binding energy of  $R_3BPR'_3$  are expected to be favorable for the stabilization of  $[R_3BH^-][HPR'_3^+]$ . Another point corresponds to the activation energy. For both types of reactions,  $CLP(FLP) + H_2$ , the reactivity of CLP or FLP is controlled mainly by the binding energy rather than the electronic effect. As a consequence, the frustration energy lowers the energy barrier and increases the stability of  $[R_3BH^-][HPR'_3^+]$ . In general, the binding energy increases upon the increasing of the acidity of  $R_3B$  and the basicity of  $PR'_3$  until they are strongly influenced by steric factors.

**Acknowledgment.** The research in Xiamen is supported by the Natural Science Foundation of China (No 20533020, 20873106) and the National Basic Research Program of China (204CB719902).

## References and Notes

(1) (a) Scheiner, S. *Annu. Rev. Phys. Chem.* **1994**, *45*, 23. (b) Scheiner, S. *Hydrogen Bonding: A Theoretical Perspective*; Oxford University Press:

New York, 1997; (c) Jeffrey, G. A. *An Introduction to Hydrogen Bonding*; Oxford University Press: New York, 1997; (d) Desiraju, G. R.; Steiner, T. *The Weak Hydrogen Bond In Structural Chemistry and Biology*; Oxford University Press: New York, 2001.

(2) (a) Wessel, J.; Lee, J. C.; Peris, E.; Yap, G. P. A.; Fortin, J. B.; Ricci, J. S.; Sini, G.; Albinati, A.; Koetzle, T. F.; Eisenstein, O.; Rheingold, A. L.; Crabtree, R. H. *Angew. Chem., Int. Ed.* **1995**, *34*, 2507. (b) Lough, A. J.; Park, S.; Ramachandran, R.; Morris, R. H. *J. Am. Chem. Soc.* **1994**, *116*, 8356. (c) Lee, J. C., Jr.; Peris, E.; Rheingold, A. L.; Crabtree, R. H. *J. Am. Chem. Soc.* **1994**, *116*, 11014. (d) Bakhmutova, E. V.; Bakhmutov, V. I.; Belkova, N. V.; Besora, M.; Epstein, L. M.; Lledos, A.; Nikonov, G. I.; Shubina, E. S.; Tomas, J.; Vorontsov, E. V. *Chem.—Eur. J.* **2004**, *10*, 661. (e) Grabowski, S. J.; Sokalski, W. A.; Leszczynski, J. *Chem. Phys.* **2007**, *337*, 68. (f) Bakhmutov, V. I. *Dihydrogen Bond: Principles, Experiments, and Applications*; Wiley: New York, 2008.

(3) (a) Richardson, T. B.; de Gala, S.; Crabtree, R. H.; Siegbahn, P. E. M. *J. Am. Chem. Soc.* **1995**, *117*, 12875. (b) Crabtree, R. H.; Siegbahn, P. E. M.; Eisenstein, O.; Rheingold, A. L.; Koetzle, T. F. *Acc. Chem. Res.* **1996**, *29*, 348.

(4) Crabtree, R. H. *Science* **1998**, *282*, 2000.

(5) Custelcean, R.; Jackson, J. E. *Chem. Rev.* **2001**, *101*, 1963.

(6) (a) Epstein, L. M.; Shubina, E. S. *Coord. Chem. Rev.* **2002**, *231*, 165. (b) Belkova, N. V.; Shubina, E. S.; Epstein, L. M. *Acc. Chem. Res.* **2005**, *38*, 624.

(7) Grabowski, S. J.; Sokalski, W. A.; Leszczynski, J. *J. Phys. Chem. A* **2005**, *109*, 4331.

(8) (a) Ayllón, J. A.; Gervaux, C.; Sabo-Etienne, S.; Chaudret, B. *Organometallics* **1997**, *16*, 2000. (b) Shubina, E. S.; Belkova, N. V.; Bakhmutova, E. V.; Vorontsov, E. V.; Bakhmutov, V. I.; Ionidis, A. V.; Bianchini, C.; Marvelli, L.; Peruzzini, M.; Epstein, L. M. *Inorg. Chim. Acta* **1998**, *280*, 302. (c) Gründemann, S.; Ulrich, S.; Limbach, H.-H.; Golubev, N. S.; Denisov, G. S.; Epstein, L. M.; Sabo-Etienne, S.; Chaudret, B. *Inorg. Chem.* **1999**, *38*, 2550. (d) Cayuela, E.; Jalon, F. A.; Manzano, B. R.; Espino, G.; Weissensteiner, W.; Mereiter, K. *J. Am. Chem. Soc.* **2004**, *126*, 7049.

(9) Klooster, W. T.; Koetzle, T. F.; Siegbahn, P. E. M.; Richardson, T. B.; Crabtree, R. H. *J. Am. Chem. Soc.* **1999**, *121*, 6337.

(10) Epstein, L. M.; Shubina, E. S.; Bakhmutova, E. V.; Saitkulova, L. N.; Bakhmutov, V. I.; Chistyakov, A. L.; Stankevich, I. V. *Inorg. Chem.* **1998**, *37*, 3013.

(11) Belkova, N. V.; Filippov, O. A.; Filin, A. M.; Teplitskaya, L. N.; Shmyrova, Y. V.; Gavrilenko, V. V.; Golubinskaya, L. M.; Bregadze, V. I.; Epstein, L. M.; Shubina, E. S. *Eur. J. Inorg. Chem.* **2004**, 3453.

(12) Marincean, S.; Jackson, J. E. *J. Phys. Chem. A* **2004**, *108*, 5521.

(13) Filippov, O. A.; Filin, A. M.; Tsupreva, V. N.; Belkova, N. V.; Lledos, A.; Ujaque, G.; Epstein, L. M.; Shubina, E. S. *Inorg. Chem.* **2006**, *45*, 3086.

(14) (a) Kulkarni, S. A. *J. Phys. Chem. A* **1998**, *102*, 7704. (b) Kulkarni, S. A.; Srivastava, A. K. *J. Phys. Chem. A* **1999**, *103*, 2836.

(15) (a) Solimannejad, M.; Alkorta, I. *J. Phys. Chem. A* **2006**, *110*, 10817. (b) Li, J. S.; Zhao, F.; Jing, F. Q. *J. Chem. Phys.* **2002**, *116*, 25.

(16) (a) Singh, P. C.; Patwari, G. N. *Chem. Phys. Lett.* **2006**, *419*, 5. (b) Singh, P. C.; Patwari, G. N. *Chem. Phys. Lett.* **2006**, *419*, 265.

(17) (a) Grabowski, S. J. *Chem. Phys. Lett.* **1999**, *312*, 542. (b) Zhu, W. L.; Puah, C. M.; Tan, X. J.; Jiang, H. L.; Chen, K. X. *J. Phys. Chem. A* **2001**, *105*, 426. (c) Grabowski, S. J. *J. Phys. Chem. A* **2000**, *104*, 5551. (d) Cybulski, H.; Pecul, M.; Sadlej, J. *J. Chem. Phys.* **2003**, *119*, 5094. (e) Grabowski, S. J.; Sokalski, W. A.; Leszczynski, J. *J. Phys. Chem. A* **2004**, *108*, 5823. (f) Wu, Y.; Feng, L.; Zhang, X. D. *THEOCHEM* **2008**, *851*, 294.

(18) Alkorta, I.; Elguero, J.; Mo, O.; Yanez, M.; Del Bene, J. E. *J. Phys. Chem. A* **2002**, *106*, 9325.

(19) (a) Gilli, P.; Bertolasi, V.; Pretto, L.; Ferretti, V.; Gilli, G. *J. Am. Chem. Soc.* **2004**, *126*, 3845. (b) Gora, R. W.; Grabowski, S. J.; Leszczynski, J. *J. Phys. Chem. A* **2005**, *109*, 6397.

(20) Grabowski, S. J.; L., R. T.; Leszczynski, J. *Chem. Phys. Lett.* **2004**, *386*, 44.

(21) *Recent Advances in Hydride Chemistry*; Peruzzini, M., Poli, R., Eds.; Elsevier: Amsterdam, The Netherlands, 2001.

(22) Hamilton, C. W.; Baker, R. T.; Staubitz, A.; Manners, I. *Chem. Soc. Rev.* **2009**, *38*, 279.

(23) Bakhmutov, V. I. *Eur. J. Inorg. Chem.* **2005**, 2005, 245.

(24) (a) Welch, G. C.; Juan, R. R. S.; Masuda, J. D.; Stephan, D. W. *Science* **2006**, *314*, 1124. (b) McCahill, J. S. J.; Welch, G. C.; Stephan, D. W. *Angew. Chem., Int. Ed.* **2007**, *46*, 4968. (c) Welch, G. C.; Cabrera, L.; Chase, P. A.; Hollink, E.; Masuda, J. D.; Wei, P. R.; Stephan, D. W. *Dalton Trans.* **2007**, 3407.

(25) Welch, G. C.; Stephan, D. W. *J. Am. Chem. Soc.* **2007**, *129*, 1880.

(26) Rokob, T. A.; Hamza, A.; Stirling, A.; Soos, T.; Papai, I. *Angew. Chem., Int. Ed.* **2008**, *47*, 2435.

(27) Guo, Y.; Li, S. H. *Inorg. Chem.* **2008**, *47*, 6212.

(28) Nguyen, V. S.; Matus, M. H.; Grant, D. J.; Nguyen, M. T.; Dixon, D. A. *J. Phys. Chem. A* **2007**, *111*, 8844.

- (29) (a) Mo, Y.; Gao, J. *J. Phys. Chem. A* **2001**, *105*, 6530. (b) Mo, Y.; Subramanian, G.; Ferguson, D. M.; Gao, J. *J. Am. Chem. Soc.* **2002**, *124*, 4832. (c) Nakashimaa, K.; Zhang, X.; Xiang, M.; Lin, Y.; Lin, M.; Mo, Y. *J. Theory Comput. Chem.* **2008**, *7*, 639.
- (30) Mo, Y.; Gao, J.; Peyerimhoff, S. D. *J. Chem. Phys.* **2000**, *112*, 5530.
- (31) Mo, Y. *J. Mol. Mod.* **2006**, *12*, 665.
- (32) Mo, Y.; Song, L.; Lin, Y. *J. Phys. Chem. A* **2007**, *111*, 8291.
- (33) Alkorta, I.; Rozas, I.; Elguero, J. *J. Chem. Soc. Rev.* **1998**, *27*, 163.
- (34) (a) Alkorta, I.; Elguero, J. *J. Phys. Chem. A* **1999**, *103*, 272. (b) Alkorta, I.; Rozas, I.; Mo, O.; Yanez, M.; Elguero, J. *J. Phys. Chem. A* **2001**, *105*, 7481. (c) Barnes, A. J.; Legon, A. C. *J. Mol. Struct.* **1998**, *448*, 101. (d) Heidrich, D.; Hommes, N. J. R. V.; Schleyer, P. v. R. *J. Comput. Chem.* **1993**, *14*, 1149. (e) Hunt, S. W.; Higgins, K. J.; Craddock, M. B.; Brauer, C. S.; Leopold, K. R. *J. Am. Chem. Soc.* **2003**, *125*, 13850. (f) Jordan, M. J. T.; Del Bene, J. E. *J. Am. Chem. Soc.* **2000**, *122*, 2101. (g) Legon, A. C. *J. Chem. Soc. Rev.* **1993**, *22*, 153. (h) Ramos, M.; Alkorta, I.; Elguero, J.; Golubev, N. S.; Denisov, G. S.; Benedict, H.; Limbach, H. H. *J. Phys. Chem. A* **1997**, *101*, 9791. (i) Rozas, I.; Alkorta, I.; Elguero, J. *J. Am. Chem. Soc.* **2000**, *122*, 11154. (j) Solans-Monfort, X.; Sodupe, M.; Mo, O.; Yanez, M.; Elguero, J. *J. Phys. Chem. B* **2005**, *109*, 19301.
- (35) Boys, S. F.; Bernardi, F. *Mol. Phys.* **1970**, *19*, 553.
- (36) Reed, A. E.; Curtiss, L. A.; Weinhold, F. *J. Chem. Phys.* **1988**, *88*, 899.
- (37) (a) Kitaura, K.; Morokuma, K. *Int. J. Quantum Chem.* **1976**, *10*, 325. (b) Stevens, W. J.; Fink, W. H. *J. Chem. Phys. Lett.* **1987**, *139*, 15. (c) Gutowski, M.; Piela, L. *Mol. Phys.* **1988**, *64*, 337. (d) Cybulski, S. M.; Scheiner, S. *J. Chem. Phys. Lett.* **1990**, *166*, 57. (e) Moszynski, R.; Heijmen, T. G. A.; Jeziorski, B. *Mol. Phys.* **1994**, *88*, 741. (f) Glendening, E. D.; Streitwieser, A. *J. Chem. Phys.* **1994**, *100*, 2900. (g) Chen, W.; Gordon, M. S. *J. Phys. Chem.* **1996**, *100*, 14316. (h) van der Vaart, A.; Merz, K. M., Jr. *J. Phys. Chem. A* **1999**, *103*, 3321. (i) Bickelhaupt, F. M.; Baerends, E. J. In *Reviews in Computational Chemistry*; Lipkowitz, K. B., Boyd, D. B., Eds.; Wiley: New York, 2000; Vol. 15, pp 1. (j) Frenking, G.; Wichmann, K.; Frohlich, N.; Loschen, C.; Lein, M.; Frunzke, J.; Rayon, V. M. *Coord. Chem. Rev.* **2003**, *238*, 238.
- (38) Mo, Y. *J. Chem. Phys.* **2003**, *119*, 1300.
- (39) Schmidt, M. W.; Baldrige, K. K.; Boatz, J. A.; Elbert, S. T.; Gordon, M. S.; Jensen, J. J.; Koseki, S.; Matsunaga, N.; Nguyen, K. A.; Su, S.; Windus, T. L.; Dupuis, M.; Montgomery, J. A. *J. Comput. Chem.* **1993**, *14*, 1347.
- (40) Khaliullin, R. Z.; Cobar, E. A.; Lochan, R. C.; Bell, A. T.; Head-Gordon, M. *J. Phys. Chem. A* **2007**, *111*, 8753.
- (41) Curtiss, L. A.; Redfern, P. C.; Raghavachari, K.; Rassolov, V.; Pople, J. A. *J. Chem. Phys.* **1999**, *110*, 4703.
- (42) Frisch, M. J.; Trucks, G. W.; Schlegel, H. B.; Scuseria, G. E.; Robb, M. A.; Cheeseman, J. R.; Montgomery, J., J. A.; Vreven, T.; Kudin, K. N.; Burant, J. C.; Millam, J. M.; Iyengar, S. S.; Tomasi, J.; Barone, V.; Mennucci, B.; Cossi, M.; Scalmani, G.; Rega, N.; Petersson, G. A.; Nakatsuji, H.; Hada, M.; Ehara, M.; Toyota, K.; Fukuda, R.; Hasegawa, J.; Ishida, M.; Nakajima, T.; Honda, Y.; Kitao, O.; Nakai, H.; Klene, M.; Li, X.; Knox, J. E.; Hratchian, H. P.; Cross, J. B.; Bakken, V.; Adamo, C.; Jaramillo, J.; Gomperts, R.; Stratmann, R. E.; Yazyev, O.; Austin, A. J.; Cammi, R.; Pomelli, C.; Ochterski, J. W.; Ayala, P. Y.; Morokuma, K.; Voth, G. A.; Salvador, P.; Dannenberg, J. J.; Zakrzewski, V. G.; Dapprich, S.; Daniels, A. D.; Strain, M. C.; Farkas, O.; Malick, D. K.; Rabuck, A. D.; Raghavachari, K.; Foresman, J. B.; Ortiz, J. V.; Cui, Q.; Baboul, A. G.; Clifford, S.; Cioslowski, J.; Stefanov, B. B.; Liu, G.; Liashenko, A.; Piskorz, P.; Komaromi, I.; Martin, R. L.; Fox, D. J.; Keith, T.; Al-Laham, M. A.; Peng, C. Y.; Nanayakkara, A.; Challacombe, M.; Gill, P. M. W.; Johnson, B.; Chen, W.; Wong, M. W.; Gonzalez, C.; Pople, J. A. *Gaussian 03*, revision C.02; Gaussian, Inc.: Wallingford, CT, 2004.
- (43) Grimme, S. *J. Chem. Phys.* **2003**, *118*, 9095.
- (44) Ahlrichs, R.; Bär, M.; Haser, M.; Horn, H.; Kölmel, C. *J. Chem. Phys. Lett.* **1989**, *162*, 165.
- (45) (a) Biegler-König, F.; Schönbohm, J. *J. Comput. Chem.* **2002**, *23*, 1489. (b) Biegler-König, F.; Schönbohm, J.; Bayles, D. *J. Comput. Chem.* **2001**, *22*, 545.
- (46) Bader, R. F. W. *Atoms in Molecules. A Quantum Theory*; Oxford University Press: New York, 1990.
- (47) Singh, P. C.; Patwari, G. N. *J. Phys. Chem. A* **2007**, *111*, 3178.
- (48) Hobza, P.; Havlas, Z. *J. Chem. Phys.* **2000**, *112*, 4253.
- (49) Bader, R. F. W.; Cheeseman, J. R.; Laidig, K. E.; Wiberg, K. B.; Breneman, C. *J. Am. Chem. Soc.* **1990**, *112*, 6530.
- (50) (a) Koch, U.; Popelier, P. L. A. *J. Phys. Chem.* **1995**, *99*, 9747. (b) Popelier, P. L. A. *J. Phys. Chem. A* **1998**, *102*, 1873.
- (51) (a) Li, X.; Liu, L.; Schlegel, H. B. *J. Am. Chem. Soc.* **2002**, *124*, 9639. (b) Cubero, E.; Orozco, M.; Hobza, P.; Luque, F. J. *J. Phys. Chem. A* **1999**, *103*, 6394. (c) Joseph, J.; Jemmis, E. D. *J. Am. Chem. Soc.* **2007**, *129*, 4620.
- (52) Alabugin, I. V.; Manoharan, M.; Peabody, S.; Weinhold, F. *J. Am. Chem. Soc.* **2003**, *125*, 5973.
- (53) Yang, Y.; Zhang, W. *THEOCHEM* **2007**, *814*, 113.
- (54) Bent, H. A. *J. Chem. Phys.* **1961**, *35*, 275.
- (55) (a) Crabtree, R. H. *Acc. Chem. Res.* **1990**, *23*, 95. (b) Kubas, G. J. *Acc. Chem. Res.* **1988**, *21*, 120.
- (56) Tague, T. J., Jr.; Andrews, L. *J. Am. Chem. Soc.* **1994**, *116*, 4970.
- (57) Schreiner, P. R.; Schaefer, H. F., III; Schleyer, P. v. R. *J. Chem. Phys.* **1994**, *101*, 7625.
- (58) (a) Hoheisel, C.; Kutzelnigg, W. *J. Am. Chem. Soc.* **1975**, *97*, 6970. (b) Stanton, J. F.; Lipscomb, W. N.; Bartlett, R. J. *J. Am. Chem. Soc.* **1989**, *111*, 5173. (c) Kim, K. H.; Kim, Y. *J. Chem. Phys.* **2004**, *120*, 623.
- (59) Schuurman, M. S.; Allen, W. D.; Schleyer, P. v. R.; Schaefer, H. F., III *J. Chem. Phys.* **2005**, *122*, 104302.